IEEE Access
Multidisciplinary ⋮ Rapid Review ⋮ Open Access Journal

Received 22 December 2022, accepted 18 January 2023, date of publication 30 January 2023, date of current version 9 February 2023.

Digital Object Identifier 10.1109/ACCESS.2023.3240573

RESEARCH ARTICLE

Fast Finite-State Predictive Current Control of Electric Drives

MANUEL R. ARAHAL[1], FEDERICO BARRERO[2], MANUEL G. SATUÉ[1], AND MARIO BERMÚDEZ[3]

[1]Departamento de Ingeniería de Sistemas y Automática, University of Seville, 41004 Seville, Spain
[2]Departamento de Ingeniería Electrónica, University of Seville, 41004 Seville, Spain
[3]Departamento de Ingeniería Eléctrica, University of Seville, 41004 Seville, Spain

Corresponding author: Manuel G. Satué (mgarrido16@us.es)

This work is part of the Grant TED2021-129558B-C22 funded by MCIN/AEI/10.13039/501100011033 and by the "European Union NextGenerationEU/PRTR". Also, the authors want to thank the support provided by project I+D+i / PID2021-125189OB-I00, funded by MCIN/AEI/10.13039/501100011033/ by "ERDF A way of making Europe."

ABSTRACT This work presents a novel optimization method for the implementation of finite-state model-based predictive current controllers in electrical drives. The proposal avoids the usual exhaustive search to find the control action, reducing the computational burden. The method is based on physical considerations of the power converter voltage vectors and is easy to implement on digital signal processors. The proposal is applied to a five-phase induction machine. Experimental results are compared with those obtained by a standard model-based controller, showing the feasibility of the proposal and the improvements in terms of sampling time reduction and control accuracy.

INDEX TERMS Induction machines, multi-phase systems, predictive control, sampling time reduction, voltage vectors.

I. INTRODUCTION

Variable speed drives based mainly on three-phase systems are used in many applications [1], [2]. Multi-phase drives are an attractive alternative [3], where the extra number of phases can benefit from new control approaches. This is the case of Model Predictive Control (MPC) when used for direct digital control of the Voltage Source Inverter (VSI) states [4]. In this configuration, an outer feedback loop is used for speed/torque tracking; then, instead of a modulation block, an inner feedback loop is used for stator current tracking [5]. The inner loop is generally known as a finite-control-state MPC (FCSMPC). It was originally developed for three-phase drives; however, it has found widespread use in n-phase drives, with $n > 3$ and, in particular, for high power applications that benefit from power splitting and inherent fault tolerance capabilities [6], [7], [8], [9]. The intuitive and flexible control formulation of MPC [10] allows to treat extra phases with ease, considering torque-producing and harmonic sub-spaces [11]. However, the optimization phase in FCSMPC is based on an exhaustive exploration procedure, which evaluates all allowed voltage vectors. This number is greater for larger n, thus a higher computational cost is found.

For three-phase systems long prediction horizons [12] can be achieved. In the multi-phase case the number of configurations increases exponentially with n, requiring the use of more advanced and complex hardware, increasing the sampling period, or limiting the number of configurations [13], [14]. Increasing the complexity of the hardware increases the cost of the controller. On the other hand, increasing the sampling period causes current tracking to deteriorates. The use of limited VSI configurations is usually the most attractive alternative, not only because it reduces the computational cost of FCSMPC but also because it can increase the usage of the DC link and decrease currents in harmonic planes (non-torque producing) [15]. In such strategies, the Voltage Vectors (VV) that the VSI can produce are not considered

The associate editor coordinating the review of this manuscript and approving it for publication was Jiefeng Hu.

in full; for instance, 12 VV can be used to drive a 5-phase system instead of the full set containing 32 VV. These ideas are closely related to virtual voltage vector (VVV) concept, which has been used to obtain zero average $x - y$ voltages while reducing the number of candidate VV [16]. However, the use of DC links with VVV is diminished. Some alternatives constitute groups of applicable VV for accurate modulation or to improve the utilization of the DC link. For example, only large vectors are considered in [17] to eliminate third harmonic components. Similarly, in [18] a maximum of 4 VV instead of 19 is used for a permanent magnet motor. In [19] a four-dimensional control set with optimal operating time is used for a seven-phase IM. In [20], one zero VV and two active VV are selected by evaluating a cost function for each switching state allowed of a 9-phase inverter. Similarly, a multi-vector approach is used in [21] to speed up the computations in FCSMPC of a nine-phase drive.

Regarding the problem of reducing the computational cost of MPC methods, the concept of Explicit MPC (EMPC) must be considered [22]. This type of methods transforms a quadratic programming problem (on-line optimization) into several local sub-problems that are valid for some regions of the operating space but can be pre-computed offline. In this way, the real-time implementation is facilitated because it only involves for the control law the determination of the actual region by looking into a pre-computed table. The main difficulties of the proposal arise from the division of the operating space into regions in the off-line design stage and from the amount of computation needed for the on-line determination of the actual region. However, the EMPC method has been applied in the field of electric drive research. For instance, the EMPC technique is considered for permanent magnet synchronous motors in [23] and [24], where pre-computed control laws represented by parameterized gains are provided, or in [25], where a continuous control set MPC is considered for a synchronous motor and the quadratic programming problem is solved online using an active-set determination algorithm.

Other efforts have appeared in the literature dealing with systems other than multi-phase drives. For instance, in [26] a priority sorting method is used to eliminate redundant computations for a multi-level converter. In [27] a dual-stage MPC method uses an optimized search space approach also for a multi-level converter. The Diophantine equations for the selection of the optimal control input are used in [28] to replace the conventional minimization. In [29] the number of iterations required for the optimization phase is reduced by considering the deadbeat concept and exclusion of undesired switching states; the method is applied to an active neutral point clamped topology. In [30] a fast, policy iteration based sub-optimal solver is applied to the FCSMPC of high–precision power amplifiers and buck–boost DC–DC power converters. Similar ideas have been used with direct matrix converters, where a pre-selection of switching states is made in [31]. Other researchers have used a reduction in the switching state combination of the inverter to attain shorter sampling periods and avoid the need for a double prediction that characterizes FCSMPC. For example, the current control of the three-level neutral point clamped inverter is tackled in [32], where the current error and the capacitor voltage balancing are considered dividing the space vector set into sectors. Similarly, a three-dimensional space vector is considered in [33] for a three-phase three-level four-wire neutral point clamped inverter, where Cartesian coordinates are used to simplify the controller implementation.

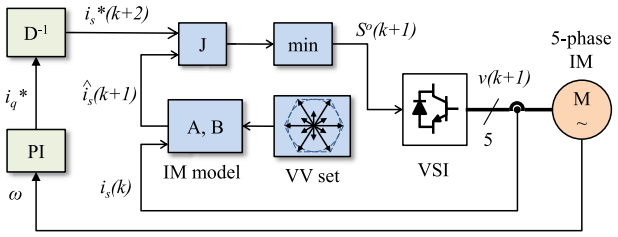

FIGURE 1. Diagram of the FCSMPC technique for the five-phase IM electric drive.

A. CONTRIBUTIONS

In this work, a novel optimization method is proposed to simplify, computationally speaking, the implementation of the FCSMPC technique. Similarly to the EMPC concept, the method aims at a faster implementation of the controller, avoiding the exhaustive search to find the optimum VV to be applied to the power converter over the available number of VSI configurations. However, there is no need for performing a complex multi-point linearization of the machine model, contrary to the EMPC technique. Insights on the electrical machine are used to obtain the optimal VV avoiding the exhaustive search. The distance between the desired stator current at $(k + 2)$ and a prediction when no control action is applied is the key to derive a table of optimal control actions that can be obtained from a pre-computed table.

The performance of the proposed algorithm is analyzed using a real five-phase drive and a Digital Signal Processor (DSP), where the implementation is done avoiding the use of trigonometric functions. Experimental results are provided to show the feasibility of the proposal and to analyze its properties in terms of robustness against parameter excursions and influence of the sampling period.

The paper is organized as follows. Section II revisits the FCSMPC control structure for reference. The proposal is then introduced in Section III, where the implementation algorithm and configuration parameters are detailed. Section IV provides the experimental results in a laboratory setup and section summarizes the conclusions.

II. CONTROL SCHEME

The most common application of FCSMPC is shown in Fig. 1, where an outer feedback loop based on an indirect field-oriented control technique is used for speed/torque

regulation [13]. The inner current regulators are replaced by the FCSMPC controller, which regulates the stator current and generates the switching state in the power converter. A discrete IM model is used to predict the stator currents for the next sampling period and then is used repeatedly for each possible voltage vector to obtain the best VSI configuration to be applied. The basic FCSMPC configuration uses a cost function J that penalizes deviations of the stator currents from their references.

At each sampling time, the VSI configuration produces stator voltages in the $\alpha-\beta$ and $x-y$ planes, $v = \left(v_{s\alpha},\ v_{s\beta},\ v_{sx},\ v_{sy}\right)$ (V), which can be calculated using the expression $v = V_{DC}STM$, where V_{DC} is the DC link voltage, S is the VSI state, T is the VSI connectivity matrix and M is a coordinate transformation matrix. The above matrices are given by:

$$T = \frac{1}{5}\begin{pmatrix} 4 & -1 & -1 & -1 & -1 \\ -1 & 4 & -1 & -1 & -1 \\ -1 & -1 & 4 & -1 & -1 \\ -1 & -1 & -1 & 4 & -1 \\ -1 & -1 & -1 & -1 & 4 \end{pmatrix} \tag{1}$$

$$M = \frac{2}{5}\begin{pmatrix} 1 & \cos\vartheta & \cos 2\vartheta & \cos 3\vartheta & \cos 4\vartheta \\ 0 & \sin\vartheta & \sin 2\vartheta & \sin 3\vartheta & \sin 4\vartheta \\ 1 & \cos 2\vartheta & \cos 4\vartheta & \cos\vartheta & \cos 3\vartheta \\ 0 & \sin 2\vartheta & \sin 4\vartheta & \sin\vartheta & \sin 3\vartheta \\ 1/2 & 1/2 & 1/2 & 1/2 & 1/2 \end{pmatrix}. \tag{2}$$

In FCSMPC, a prediction of the state of the system is used to derive the control action. To this end, a discrete-time model is derived from the continuous-time machine equations. The state of the system is composed of stator currents, rotor currents, and rotor speed. For stator current control, only stator currents need to be predicted. Considering vector $i = \left(i_{s\alpha},\ i_{s\beta},\ i_{sx},\ i_{sy}\right)$ (A), then the prediction is found as

$$\hat{i}(k+1|k) = Ai(k) + Bv(k|k-1) + \hat{G}(k|k), \tag{3}$$

where $\hat{i}(k+1|k)$ (A) is an estimation of the stator currents for discrete time $k+1$ made at time k. In (3), the stator voltage produced by the VSI is denoted as $v(k|k-1)$ (V). Also, the term G (A) is added as an estimation of the effect of rotor currents on stator current dynamics (please note that rotor currents are not measured in most applications).

Another prediction must be made to account for the delay in computations, which is of the order of magnitude of the sampling period in FCSMPC. Then the two-step ahead prediction can be found as:

$$\hat{i}(k+2|k) = A\hat{i}(k+1|k) + Bv(k+1|k) + \hat{G}(k|k). \tag{4}$$

The VSI state for the next sampling period, denoted $S(k+1)$ (vector of boolean values), is done by minimizing a certain cost function J. This function can hold different terms corresponding to different control objectives. The simplest one is given below

$$J(k+2) = \|\hat{e}_{\alpha\beta}(k+2)\|^2, \tag{5}$$

where $\hat{e}_{\alpha\beta}(k+2) = i^*_{\alpha\beta}(k+2) - \hat{i}_{\alpha\beta}(k+2)$ (A) is a prediction of the tracking error in the $\alpha-\beta$ sub-space. Reference values are obtained from the i^*_q (A) value provided by the outer loop (see the diagram in Fig. 1). Recall that the desired trajectories for the stator currents are sinusoidal, with amplitude $I^*_s = \sqrt{i^{*2}_{sd} + i^{*2}_{sq}}$ (A) and with an electrical frequency ω_e (rad/s) related to the mechanical speed and slip. In this way, the references in the torque producing plane are $i^*_{s\alpha}(t) = I^*_s \sin\omega_e t$, $i^*_{s\beta}(t) = I^*_s \cos\omega_e t$, and in the harmonic plane $i^*_{sx}(t) = 0$, $i^*_{sy}(t) = 0$.

The minimization of the cost function provides the optimal VSI state for $(k+1)$. In mathematical notation:

$$S^o(k+1) = \underset{\mathbf{VV}}{\operatorname{argmin}}\, J(k+2), \tag{6}$$

where **VV** specifies the allowed voltage vectors for the multiphase system.

III. FAST COMPUTATION OF THE VV

The proposed method considers first a prediction of the error for $k+2$ for the case where the null voltage vector is applied. This prediction considers the IM's internal dynamics and can be used to determine the amount of voltage to be applied to each axis (α, β, x, y) to cancel the error. Since exact cancellation is not possible, the method uses the prediction as a way to compute the voltage vector that the FCSMPC would select, avoiding exhaustive exploration and relying on a geometric construction. To proceed in order, first the predicted error if the null voltage vector is applied is defined as

$$\hat{i}_0(k+2) = i^*_{\alpha-\beta}(k+2) - \hat{i}(k+2|k) \tag{7}$$

where $\hat{i}(k+2|k) = A\hat{i}(k+1|k)$ (A) according to equation (3). The voltage to be used in $k+1$ to cancel this error can be calculated from eq. (4) as

$$v^*(k+1) = B^{-1}\hat{i}_0(k+2) \tag{8}$$

Now, the voltage vector that best approximates $v^*(k+1)$ (V) can be found using a table after determining the region in which this vector lies. This region determination is explained in the following. The actual values for the 5-phase VSI used in the experimental section are given in Fig. 2.

The region determination algorithm is given below. Please note that the evaluation of $B^{-1}\hat{i}_0(k+2)$ can be avoided, since the multiplication by B^{-1} is akin to a scale factor. Thus, the algorithm can work with the quantity $\hat{i}_0(k+2)$ directly, for ease of presentation, the quantity will be denoted as $p^0 = \hat{i}_0(k+2)$.

1) Compute the norm $\rho = |\ (p^0_\alpha, p^0_\beta)\ |$. Four cases arise: 1) $\rho \geq G_L$, 2) $G_M < \rho \leq G_L$, 3) $G_S < \rho \leq G_M$, and 4) $\rho < G_S$.
2) Compute Q, the quadrant of (p^0_α, p^0_β).
3) Compute the ratio $\tau = |\ p^0_\beta / p^0_\alpha\ |$. Determine the case: A) for $\tau \geq U_1$, B) for $U_2 \leq \tau < U_1$, and C) for $\tau < U_2$.
4) Compute the voltage vector index according to τ, ρ and Q as indicated in Table 1.

TABLE 1. Voltage Vectors for each case.

Cases		Quadrant			
τ	ρ	1	2	3	4
A	1	28	12	3	19
A	2	8	30	23	1
A	3	20	13	11	18
A	4	0	0	0	0
B	1	24	14	7	17
B	2	29	4	2	27
B	3	26	10	5	21
B	4	0	0	0	0
C	1	25	6	6	25
C	2	16	15	15	16
C	3	9	22	22	9
C	4	0	0	0	0

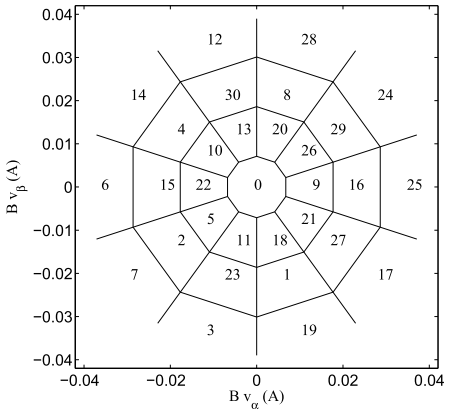

FIGURE 2. Regions for each VV for the 5-phase VSI indicated by an index from 0 to 31.

The parameters U_1 and U_2 are based on geometric considerations given the ten-fold symmetry of the regions, resulting in $U_1 = 1.3764$ and $U_2 = 0.3249$. The parameters G_L, G_M, and G_S are based on the distances from the origin of the values p^0, corresponding to the large, medium and small voltage vectors. This set of parameters is machine dependent and can be computed from the equations of the model (3)-(4). They correspond to the midpoints between different VV coronas. For example, G_L is between large and medium VVs, G_M is between medium and small VVs, and G_S is between small and zero VVs. For the case analyzed, the values are $G_S = 0.0089$ (A), $G_M = 0.0234$ (A), and $G_L = 0.0340$ (A).

A. COMPUTATIONAL LOAD

The proposed method avoids the exhaustive optimization used in FCSMPC. The savings in terms of computational burden are very noticeable, specially for multi-phase systems where a larger number of voltage vectors are available (compared with the three-phase case). The reduction takes place in the optimization phase. For the A/D conversion, PI controller, delay compensation and other processes, the proposal and the standard FCSMPC bear the same burden. For this reason, the following discussion is based only on the optimization phase.

The reduction in computational effort due to the proposal is easy to grasp considering a multi-phase system where N_{VV} voltage vectors are available. For instance, for a 5-phase system there are 32 possible voltage vectors, although in some cases just a subset is used for whatever reasons. In this context, the standard FCSMPC using exhaustive optimization must obtain N_{VV} two-step ahead predictions and their correspondent values of the cost function. To obtain such values, the FCSMPC algorithm needs N_{VV} times the following: a 4×4 matrix multiplication and 2 additions of 4-element vectors (for the predictions), two vector modulus, a multiplication, and an addition (for the computation of the cost function). These requirements are much higher than those of the algorithm given in Section III, which requires, at most and regardless of the actual value of p^0, the following computations:

- Two scalar multiplications and an addition for the computation of ρ, then three comparisons to obtain the case for ρ.
- Two comparisons to find the quadrant Q.
- A division and a comparison to find τ, then two comparisons to find the case for τ.
- One access to a table to find the VV number.

In terms of computing time, a TMS320F28335 microprocessor has been used to provide the times needed by FCSMPC and by the proposal. The same microprocessor has been used in the experimental tests that will be presented later. Also, in the comparison, only the 10 large vectors provided by the VSI and the zero configurations will be used. This reduces N_{VV} from 32 to 12, providing a less favorable ground of comparison for the proposal. Fig. 3 illustrates the results. It can be seen that the standard FCSMPC needs about $9\mu s$ for the cost function optimization, whereas the proposal takes roughly $2.3\mu s$. The rest of processes are similar in both cases.

This means a notable reduction of the computational cost of the conventional optimization technique even for the restricted case of $N_{VV} = 12$. What is more significant, the proposal has a computational burden equivalent to that of the A/D conversion and other processes, which means that the optimization process using the proposal is no longer heavy from a computational cost perspective. This can favor the industrial application of MPC in variable-speed drives in the future even with microprocessors of moderate power.

B. SIMULATION RESULTS

The proposed method is compared now with the standard FCSMPC using a five-phase IM as a test-bed. The parameters are the same as in the experimental setup that will be introduced later. For the assessment of the variable-speed drive, the Root Mean Squared tracking error is considered. This quantity is computed as

$$E_{\alpha-\beta} = \sqrt{\frac{1}{(k_2 - k_1 + 1)} \sum_{k=k_1}^{k_2} e_{\alpha\beta}^2(k)} \tag{9}$$

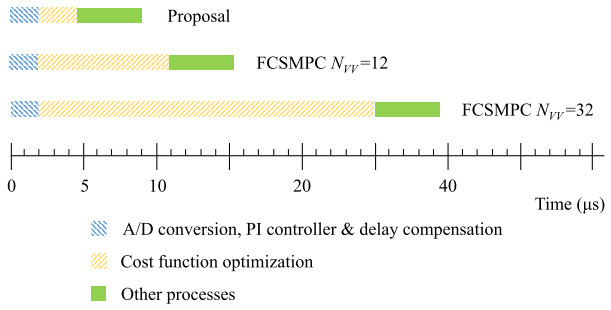

FIGURE 3. Computation times during a sampling period, using the proposal (top bar) and the standard FCSMPC (bottom bar).

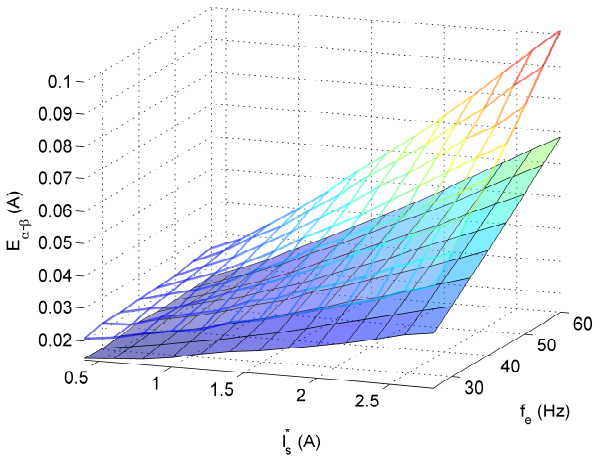

FIGURE 4. Root mean values of the control error found in simulation using the proposal (solid surface) and the standard FCSMPC approach (hollowed surface on top).

Obviously, a low value of $E_{\alpha-\beta}$ indicates better stator current tracking which is beneficial for the drive operation. Fig. 4 shows the values of $E_{\alpha-\beta}$ found by simulation in the whole operational range of the IM. The superiority of the approach is quite apparent as predicted in [34].

IV. EXPERIMENTAL RESULTS

A five-phase IM has been considered for the presentation of the method and its assessment. The main electrical and mechanical parameters that characterized the experimental test bench are detailed in Table 2, while the test bench is shown in Fig. 5. The experimental system includes two three-phase inverters (SKS-22F from Semikron), of which only five power legs are connected to the electrical machine. The DC link voltage is provided by an Argantix DC power supply. A MSK28335 control board and a Texas Instruments TMS320F28335 digital signal processor are used to implement the control algorithms.

The voltage vectors for a five-phase VSI are shown in Fig. 5. It can be seen that those lying in the outer corona in the $\alpha-\beta$ subspace (red arrows) produce the shortest content in the $x-y$ subspace. The outer corona (the ten largest VV) plus the two zero configurations can be used. This reduces N_{VV} from 32 to just 12, reducing the time required by the

TABLE 2. Parameters of the five-phase IM.

Parameter	Value	Unit
Stator resistance, R_s	12.85	Ω
Rotor resistance, R_r	4.80	Ω
Stator leakage inductance, L_{ls}	79.93	mH
Rotor leakage inductance, L_{lr}	79.93	mH
Mutual inductance, L_m	681.7	mH
Rotational inertia, J_m	0.02	kg m^2
Friction, B_m	0.0118	Nms/rad
Number of pairs of poles, P	3	-

standard FCSMPC to obtain the control signal with reduced induced $x-y$ currents. As a result of faster computations, shorter sampling times are achieved in FCSMPC and better performance indices can be obtained in the response of the closed-loop system [34]. In the following, this configuration is adopted as a benchmark (standard FCSMPC technique) for comparison purposes to state the interest of the proposal. This choice constitutes a favorable scenario for standard FCSMPC method as the proposal is not affected by the value N_{VV}.

Figure 6 shows the trajectory of the stator currents on the α axis. The experimental conditions are set by a reference mechanical speed of 750 rpm and full load torque. It can be seen that current tracking is superior in the case of the proposed method as a result of the reduction in sampling time. In this case, the standard FCSMPC is run at a sampling frequency $f_s = 20$ (kHz) ($T_s = 50\mu s$) that is a value in the range often found in the literature and that can be achieved by most DSPs. The proposed method could run much faster due to the comparatively low computing burden; however, a sampling frequency $f_s = 30$ (kHz) ($T_s = 33.3\mu s$) has been used to demonstrate its capabilities.

The control errors for each case are highlighted in Fig. 7, where it can be observed that the proposed scheme (indicated as Prop. in the legend) achieves better tracking of α currents compared to the standard FCSMPC (indicated as Std. in the legend). Similar results are obtained for β currents and are omitted for brevity.

Regarding the harmonic content for both approaches, in Fig. 8 the spectrum of phase currents is presented. The proposed method provides a spectrum that is less spread compared to the standard FCSMPC technique. Again, this result can be explained in terms of the superior tracking capability provided by the proposal, which makes the current follow the sinusoidal reference with greater accuracy, improving the content at the fundamental frequency. Please note that the broader spectrum of FCSMPC is one of the drawbacks holding back its acceptation in industry.

The proposal is also analyzed in the transient state, applying a step-load test. The results are shown in Fig. 9, where the response using the proposed method is compared with that obtained using the conventional FCSMPC technique. Note that the outer speed control loops use the same tuned PI. The proposed controller offers a speed regulation similar to that of the conventional FCSMPC method, reducing the ripple of the torque-producing stator current, i_{sq}.

The influence of the sampling period can be checked in Table 3, where the RMS stator current tracking error is

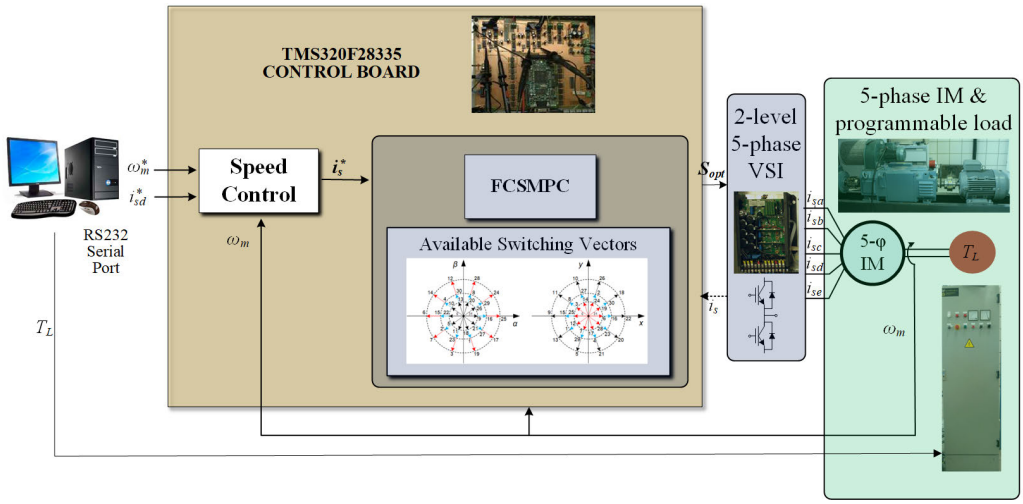

FIGURE 5. Experimental test bed based on a five-phase IM with distributed windings.

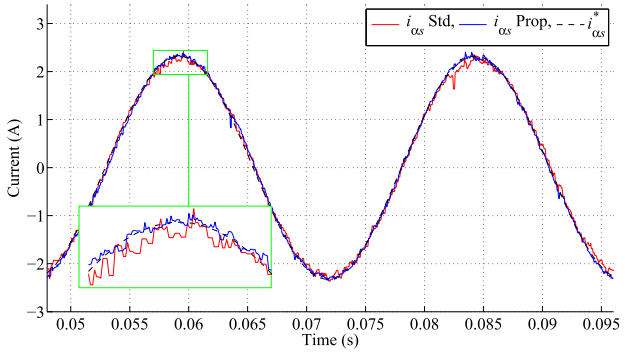

FIGURE 6. Experimental result for FCSMPC using exhaustive search (Std) and the proposed method (Prop).

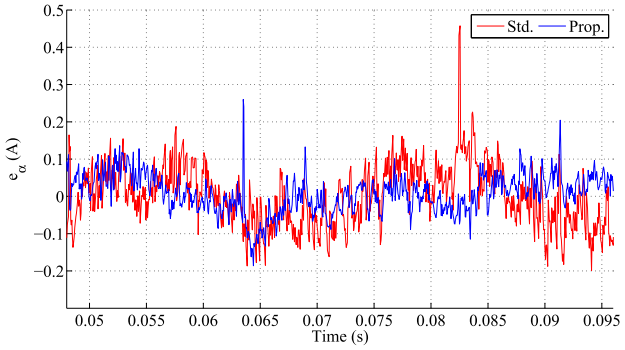

FIGURE 7. Control error for the standard FCSMPC (Std.) and the proposed method (Prop.).

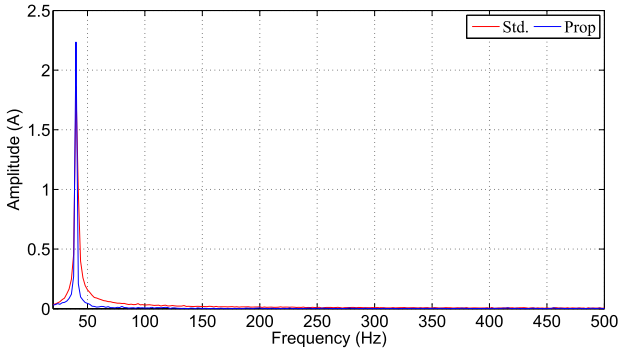

FIGURE 8. Harmonic content for FCSMPC (Std) and for the proposed method (Prop).

TABLE 3. Tracking errors for different sampling periods.

T_s	Case A	Case B	Case C
67 μ s	0.134	0.183	0.251
50 μ s	0.113	0.169	0.221
33 μ s	0.099	0.175	0.187

presented for different values of T_s. The results are the same for standard FCSMPC and for the proposal since this latter method just makes computations faster, enabling the use of lower sampling periods. The operating points corresponds to low speed and medium load (case A), medium speed and load (case B) and high speed and load (case C). It can be seen that the reduction in sampling period brings a reduction in tracking error as reported in the literature.

A. SENSITIVITY ANALYSIS

The proposed method makes computation faster, but its underlying principle is the same of the standard FCSMPC: the predictive model. The parameters used by the model can differ from the real ones [35], [36]. The effect of parameter de-tuning on performance is the same for standard FCSMPC and for the proposed method. Sensitivity of FCSMPC can be found in various papers such as [37] that deals with a five phase IM. As a reminder, Table 4 shows the results for different parametric mismatch situations. In said table, the nominal parameters (see Table 2) are not incorporated into the predictive model, instead modified values are used. These values are found as $\hat{R}_s = \gamma_1 R_s$, $\hat{R}_r = \gamma_2 R_r$, $\hat{L}_{ls} = \gamma_3 L_{ls}$, $\hat{L}_{lr} = \gamma_4 L_{lr}$, and $\hat{L}_M = \gamma_5 L_M$. The γ_i coefficients (with $i =, 1, \ldots, 5$) allow to introduce various situations. In the

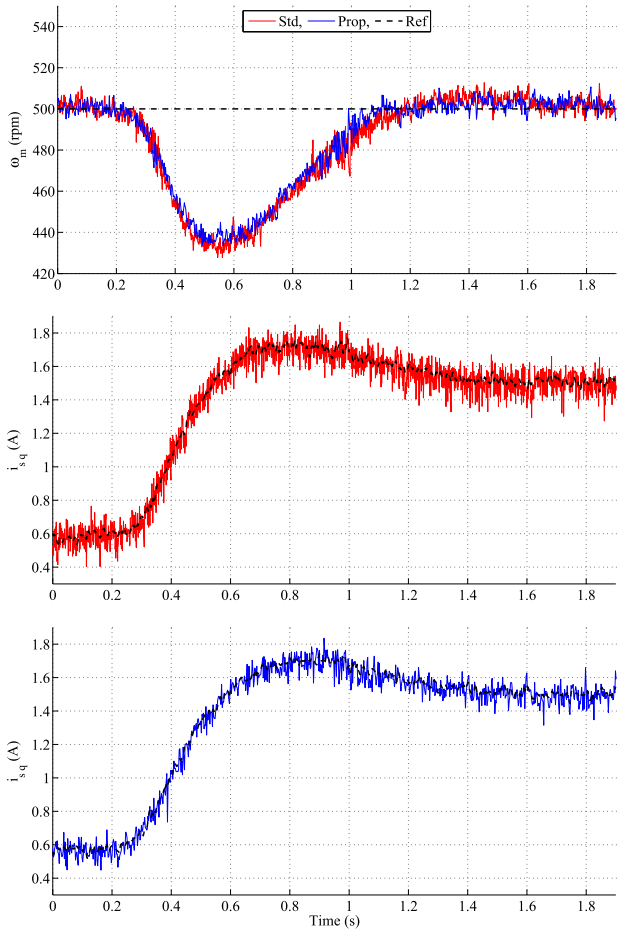

FIGURE 9. Results obtained for a step in load torque at reference speed, using the conventional FCSMPC method (Std) and the proposed technique (Prop).

TABLE 4. Degradation in RMS tracking error caused by mismatching parameters.

Change					Nominal	Mismatched
γ_1	γ_2	γ_3	γ_4	γ_5	model	model
0.5	1.0	1.0	1.0	1.0	0.1512	0.1648
2.0	1.0	1.0	1.0	1.0	0.1512	0.1527
1.0	2.0	1.0	1.0	1.0	0.1512	0.2132
1.0	1.0	2.0	1.0	1.0	0.1512	0.1981
1.5	1.5	1.5	1.5	1.5	0.1512	0.2283

table the effect of the de-tuning is can be checked comparing the performance with a nominal model and a mismatched one. It can be seen that some parameters have a stronger effect on performance as previously reported in [37].

V. CONCLUSION

A novel implementation method for FCSMPC is presented to reduce its computational requirements. The typical optimization process based on exhaustive search is replaced by a fast search algorithm based on physical insight on the voltage vectors produced by the multi-phase VSI.

Experimental results show that the method allows for a drastic reduction in sampling periods. This in turn, produces remarkable improvements using the proposal compared to the standard technique. This improvement can be even more noticeable, as the sampling time for the proposed algorithm can be significantly reduced. Although a five-phase drive has been used for the assessment, the method cab be used in other complex multi-phase and/or multilevel electric drives.

REFERENCES

[1] C. Liu, "Emerging electric machines and drives—An overview," *IEEE Trans. Energy Convers.*, vol. 33, no. 4, pp. 2270–2280, Dec. 2018.
[2] N. Güler, "Multi-objective cost function based finite control set-sliding mode control strategy for single-phase split source inverters," *Control Eng. Pract.*, vol. 122, May 2022, Art. no. 105114.
[3] E. Levi, F. Barrero, and M. J. Duran, "Multiphase machines and drives—Revisited," *IEEE Trans. Ind. Electron.*, vol. 63, no. 1, pp. 429–432, Jan. 2016.
[4] S. Borreggine, V. G. Monopoli, G. Rizzello, D. Naso, F. Cupertino, and R. Consoletti, "A review on model predictive control and its applications in power electronics," in *Proc. AEIT Int. Conf. Electr. Electron. Technol. Automot.*, Jul. 2019, pp. 1–6.
[5] M. F. Elmorshedy, W. Xu, F. F. El-Sousy, M. R. Islam, and A. A. Ahmed, "Recent achievements in model predictive control techniques for industrial motor: A comprehensive state-of-the-art," *IEEE Access*, vol. 9, pp. 58170–58191, 2021.
[6] A. Cervone and O. Dordevic, "Maximum torque per ampere algorithm for five-phase synchronous reluctance machines," *IEEE Trans. Ind. Electron.*, vol. 69, no. 10, pp. 9721–9730, Oct. 2022.
[7] R. Hammad, S. M. Dabour, and E. M. Rashad, "Asymmetrical six-phase induction motor drives based on Z-source inverters: Modulation, design, fault detection and tolerance," *Alexandria Eng. J.*, vol. 61, no. 12, pp. 10055–10070, Dec. 2022.
[8] A. G. Yepes, I. Gonzalez-Prieto, O. Lopez, M. J. Duran, and J. Doval-Gandoy, "A comprehensive survey on fault tolerance in multiphase AC drives. Part 2: Phase and switch open-circuit faults," *Machines*, vol. 10, no. 3, p. 221, Mar. 2022.
[9] P. F. C. Gonçalves, S. M. A. Cruz, and A. M. S. Mendes, "Fault-tolerant predictive current control of six-phase PMSMs with minimal reconfiguration requirements," *IEEE J. Emerg. Sel. Topics Power Electron.*, early access, Nov. 18, 2022, doi: 10.1109/JESTPE.2022.3223515.
[10] E. F. Camacho and C. Bordons, *Model Predictive Control*. London, U.K.: Springer, 2013.
[11] S. Li, J. Yang, Y. Wang, and G. Yang, "Dual closed-loop control strategy on harmonic plane for multiphase induction motor with harmonic injection based on air-gap flux orientation control," *IEEE J. Emerg. Sel. Topics Power Electron.*, vol. 10, no. 5, pp. 6101–6111, Oct. 2022.
[12] P. Karamanakos, T. Geyer, N. Oikonomou, F. Kieferndorf, and S. Manias, "Direct model predictive control: A review of strategies that achieve long prediction intervals for power electronics," *IEEE Ind. Electron. Mag.*, vol. 8, no. 1, pp. 32–43, Mar. 2014.
[13] M. Bermúdez, C. Martín, I. González-Prieto, M. J. Durán, M. R. Arahal, and F. Barrero, "Predictive current control in electrical drives: An illustrated review with case examples using a five-phase induction motor drive with distributed windings," *IET Electr. Power Appl.*, vol. 14, no. 8, pp. 1291–1310, 2020.
[14] B. Stellato, T. Geyer, and P. J. Goulart, "High-speed finite control set model predictive control for power electronics," *IEEE Trans. Power Electron.*, vol. 32, no. 5, pp. 4007–4020, May 2017.
[15] Y. Luo and C. Liu, "A simplified model predictive control for a dual three-phase PMSM with reduced harmonic currents," *IEEE Trans. Ind. Electron.*, vol. 65, no. 11, pp. 9079–9089, Nov. 2018.
[16] I. Gonzalez-Prieto, M. J. Duran, J. J. Aciego, C. Martin, and F. Barrero, "Model predictive control of six-phase induction motor drives using virtual voltage vectors," *IEEE Trans. Ind. Electron.*, vol. 65, no. 1, pp. 27–37, Jan. 2017.
[17] B. Yu, W. Song, Y. Guo, and M. S. R. Saeed, "A finite control set model predictive control for five-phase PMSMs with improved DC-link utilization," *IEEE Trans. Power Electron.*, vol. 37, no. 3, pp. 3297–3307, Mar. 2022.

[18] S. G. Petkar and T. V. Kumar, "Computationally efficient model predictive control of three-level open-end winding permanent-magnet synchronous motor drive," *IET Electr. Power Appl.*, vol. 14, no. 7, pp. 1210–1220, Jul. 2020.
[19] R. Yin and J. Yang, "Predictive current control for seven-phase induction motor based on the optimal operating time of four-dimensional vector," *IET Electr. Power Appl.*, vol. 13, no. 11, pp. 1684–1695, Nov. 2019.
[20] M. Gokdag, "Modulated predictive control to improve the steady-state performance of NSI-based electrification systems," *Energies*, vol. 15, no. 6, p. 2043, Mar. 2022.
[21] H. Wang, X. Zheng, X. Yuan, and X. Wu, "Low-complexity model-predictive control for a nine-phase open-end winding PMSM with dead-time compensation," *IEEE Trans. Power Electron.*, vol. 37, no. 8, pp. 8895–8908, Aug. 2022.
[22] A. Alessio and A. Bemporad, "A survey on explicit model predictive control," in *Nonlinear Model Predictive Control* (Lecture Notes in Control and Information Sciences), vol. 384, L. Magni, D. M. Raimondo, and F. Allgöwer, Eds. Berlin, Germany: Springer, 2009, doi: 10.1007/978-3-642-01094-1_29.
[23] M. Zhao, Y. Cao, Y. Yan, Z. Zhang, T. Shi, and C. Xia, "Weighting factors tuning method in explicit model predictive direct speed control of permanent magnet synchronous motor," in *Proc. 24th Int. Conf. Electr. Mach. Syst. (ICEMS)*, Oct. 2021, pp. 653–658.
[24] K. Belda and P. Píša, "Explicit model predictive control of PMSM drives," in *Proc. IEEE 30th Int. Symp. Ind. Electron. (ISIE)*, Jun. 2021, pp. 1–6.
[25] G. Cimini, D. Bernardini, S. Levijoki, and A. Bemporad, "Embedded model predictive control with certified real-time optimization for synchronous motors," *IEEE Trans. Control Syst. Technol.*, vol. 29, no. 2, pp. 893–900, Mar. 2021.
[26] J. Huang, B. Yang, F. Guo, Z. Wang, X. Tong, A. Zhang, and J. Xiao, "Priority sorting approach for modular multilevel converter based on simplified model predictive control," *IEEE Trans. Ind. Electron.*, vol. 65, no. 6, pp. 4819–4830, Jun. 2018.
[27] P. Guo, Z. He, Y. Yue, Q. Xu, X. Huang, Y. Chen, and A. Luo, "A novel two-stage model predictive control for modular multilevel converter with reduced computation," *IEEE Trans. Ind. Electron.*, vol. 66, no. 3, pp. 2410–2422, Mar. 2019.
[28] X. Liu, L. Qiu, J. Ma, Y. Fang, W. Wu, Z. Peng, and D. Wang, "A fast finite-level-state model predictive control strategy for sensorless modular multilevel converter," *IEEE J. Emerg. Sel. Topics Power Electron.*, vol. 9, no. 3, pp. 3570–3581, Jun. 2021.
[29] I. Harbi, M. Ahmed, J. Rodriguez, R. Kennel, and M. Abdelrahem, "Low-complexity finite set model predictive control for split-capacitor ANPC inverter with different levels modes and online model update," *IEEE J. Emerg. Sel. Topics Power Electron.*, early access, Aug. 26, 2022, doi: 10.1109/JESTPE.2022.3202238.
[30] D. Xu and M. Lazar, "On finite-control-set MPC for switched-mode power converters: Improved tracking cost function and fast policy iteration solver," in *Proc. IEEE Conf. Control Technol. Appl. (CCTA)*, Aug. 2022, pp. 1129–1134.
[31] H. Dan, Q. Zhu, T. Peng, S. Yao, and P. Wheeler, "Preselection algorithm based on predictive control for direct matrix converter," *IET Electr. Power Appl.*, vol. 11, no. 5, pp. 768–775, 2017.
[32] M.-V. Doi, B.-X. Nguyen, and N.-V. Nguyen, "A finite set model predictive current control for three-level NPC inverter with reducing switching state combination," in *Proc. IEEE 4th Int. Future Energy Electron. Conf. (IFEEC)*, Nov. 2019, pp. 1–9.
[33] S. R. Mohapatra and V. Agarwal, "A low computational cost model predictive controller for grid connected three phase four wire multilevel inverter," in *Proc. IEEE 27th Int. Symp. Ind. Electron. (ISIE)*, Jun. 2018, pp. 305–310.
[34] M. R. Arahal, F. Barrero, M. J. Durán, M. G. Ortega, and C. Martín, "Trade-offs analysis in predictive current control of multi-phase induction machines," *Control Eng. Pract.*, vol. 81, pp. 105–113, Dec. 2018.
[35] V.-Q.-B. Ngo, V.-H. Vu, V.-T. Pham, H.-N. Nguyen, P. Rodriguez-Ayerbe, S. Olaru, and H.-T. Do, "Lyapunov-induced model predictive power control for grid-tie three-level neutral-point-clamped inverter with dead-time compensation," *IEEE Access*, vol. 7, pp. 166869–166882, 2019.
[36] F. Xiao, Z. Chen, Y. Chen, and H. Liu, "A finite control set model predictive direct speed controller for PMSM application with improved parameter robustness," *Int. J. Electr. Power Energy Syst.*, vol. 143, Dec. 2022, Art. no. 108509.
[37] C. Martín, M. Bermúdez, F. Barrero, M. R. Arahal, X. Kestelyn, and M. J. Durán, "Sensitivity of predictive controllers to parameter variation in five-phase induction motor drives," *Control Eng. Pract.*, vol. 68, pp. 23–31, Nov. 2017.

MANUEL R. ARAHAL was born in Dos Hermanas, Seville, Spain, in 1966. He received the master's and Ph.D. degrees in industrial engineering from the University of Seville, in 1991 and 1996, respectively. He is currently a Full Professor with the Ingeniería de Sistemas y Automática Department, University of Seville. He has received the best paper awards from the IEEE TRANSACTIONS ON INDUSTRIAL ELECTRONICS, in 2009, and *IET Electric Power Applications*, in 2010 and 2011.

FEDERICO BARRERO received the M.Sc. and Ph.D. degrees in electrical and electronic engineering from the University of Seville, in 1992 and 1998, respectively. In 1992, he joined the Electronic Engineering Department, University of Seville, where he is currently a Full Professor. He was a recipient of the best paper awards from the IEEE TRANSACTIONS ON INDUSTRIAL ELECTRONICS, in 2009, and the *IET Electric Power Applications*, in 2010 and 2011.

MANUEL G. SATUÉ was born in Seville, Spain. He received the master's and Ph.D. degrees in industrial engineering from the University of Seville, Seville, in 2008 and 2021, respectively.

He is currently a Teaching Assistant with the Ingeniería de Sistemas y Automática Department, University of Seville. His research interests include optimization for energy systems and predictive control.

MARIO BERMÚDEZ was born in Málaga, Spain, in 1987. He received the B.Eng. degree in industrial engineering from the University of Málaga, Málaga, in 2014, and the joint Ph.D. degree in electrical/electronic engineering from Arts et Métiers ParisTech, Lille, France, and the University of Seville, Seville, Spain, in 2018. He is currently an Assistant Professor with the Department of Electrical Engineering, University of Seville.